Red Electroluminescence of Mn-doped CuAlS2 Powder and Single Crystal

Article *in* Japanese Journal of Applied Physics · June 1998

DOI: 10.1143/JJAP.37.3350

5 authors, including:

Katsuaki Sato
Tokyo University of Agriculture and Technology
289 PUBLICATIONS **3,503** CITATIONS

SEE PROFILE

Red Electroluminescence of Mn-doped $CuAlS_2$ Powder and Single Crystal

Katsu TANAKA[1,2], Yasukazu KIMURA[2,*], Shinji OKAMOTO[1], Yoji INOUE[1] and Katsuaki SATO[2]

[1]*NHK Science and Technical Research Laboratories, 1-10-11 Kinuta, Setagaya-ku, Tokyo 157-8510, Japan*

[2]*Faculty of Technology, Tokyo University of Agriculture and Technology, Koganei, Tokyo 184-8588, Japan*

(Received October 30, 1997; accepted for publication March 26, 1998)

In this paper, the first application of ternary compounds of Mn-doped $CuAlS_2$ to a new red powder electroluminescent (PEL) phosphor has been reported. The chromaticity of the emission is a high-purity red very close to that of the red-CRT phosphor. The luminance–voltage (L–V), current–voltage (I–V), and luminance–current (L–I) curves of the single crystal reveal that the excitation of red electroluminescence (EL) is caused by hot holes. The EL decay mechanism is found to be dominated by Mn–Mn pair relaxation. The DC-EL of the PEL device using Mn-doped $CuAlS_2$ was brighter than the AC-EL. This superior DC-EL performance is explained by the emitting position in the phosphor-binder layer.

KEYWORDS: Mn-doped $CuAlS_2$, red electroluminescence (EL), powder EL device, single crystal, high electric field, hot holes

1. Introduction

Powder electroluminescent (PEL) devices are flat light-emitting devices in which powder phosphors are dispersed in an organic binder. Electroluminescence (EL) occurs when a high electric field is applied to the phosphor. The PEL devices have superior features that include sheet-like flexibility, thinness, low weight, self-emission, a wide viewing angle and a fast response time. On account of these features, the practical uses of PEL devices include backlights of liquid-crystal displays, watches and signboard illuminations. Cu-activated ZnS (hereafter referred to as ZnS:Cu) phosphors, which emit blue to green light, are usually employed for these applications because their EL performance, such as brightness, efficiency and lifetime, is superior to that of other PEL phosphors.

In order to obtain full-color PEL, the development of PEL devices which emit all three primary colors, blue, green and red, is essential. The biggest problem encountered in the PEL device is the inability of the phosphor material to emit pure red EL. Till now, binary II–VI compounds such as ZnS:Sm, Na, CaS:Eu, Cl, ZnS:Cu, Mn, Cl, and $Ca_XSr_{1-X}S$:Eu alloy have been investigated for use in red PEL phosphors.[1,2]

In the present study, the authors employed the ternary compound of $CuAlS_2$:Mn for the red PEL phosphor instead of these binary compounds. The $CuAlS_2$ host material is a I–III–VI_2 chalcopyrite semiconductor with a wide energy gap of 3.55 eV[3] which is sufficiently wide to accommodate visible luminescent centers. When Mn^{2+} ions in $CuAlS_2$:Mn are photoexcited, this material exhibits red photoluminescence (PL) at around 635 nm.[4] This is a much longer wavelength than the orange emission peak around 580 nm of ZnS:Mn which is widely used as a phosphor for monochrome thin film EL devices. Furthermore, $CuAlS_2$ shows p-type conductivity, which is different from the n-type conductivity of conventional PEL host materials such as ZnS, so a unique EL excitation mechanism related to hole conduction can be expected.

We have previously fabricated an alternating current (AC)-driven EL device using a single crystal of $CuAlS_2$:Mn.[5] However, the EL was unstable and the device often showed local breakdowns. In this study, the EL properties of $CuAlS_2$:Mn were first improved by the using a direct current (DC)-driven EL device. For this trial, a metal-semiconductor-metal (MSM) diode using a single crystal was fabricated, which is equivalent to the minimum unit of a PEL device. Measurements of the DC-EL characteristics were performed with respect to the EL spectrum, *Commission Internationale de l'Eclairage* (CIE) color coordinates, luminance–voltage (L–V) curve, current–voltage (I–V) curve, luminance–current (L–I) curve and EL decay time. The EL emitting position in the crystal was also examined. Based on these results, the EL excitation mechanism of $CuAlS_2$:Mn has been intensively investigated.

The $CuAlS_2$:Mn powder phosphors were then applied to the PEL device, and the L–V curves of the PEL device were measured. The superior DC-EL performance of the PEL device is discussed.

2. Experimental

2.1 *Preparation of powder phosphors and single crystals*

2.1.1 *Powder phosphors*

A 1 wt% Mn-doped $CuAlS_2$ polycrystalline compound was prepared by direct melting of the constituent elements (Cu, Al, S: 99.9999%, Mn: 99.999%) in a boron nitride (BN) crucible. The crucible was held in a sealed and evacuated (about 10^{-6} Torr) silica ampoule. The compound was synthesized by holding the ampoule at a temperature of 1300°C for 2 days. The powdered phosphor was obtained by crushing the as-grown bulk compound, and used for the fabrication of the PEL device.

2.1.2 *Single crystal*

The Mn-doped $CuAlS_2$ single crystals were grown by the chemical vapor transport (CVT) technique using iodine as the transporting agent. The material used for CVT was the Mn-doped $CuAlS_2$ powder described in §2.1.1. The starting material was sealed in an evacuated (about 10^{-6} Torr) silica ampoule with 10 mg/cm^3 of iodine. The ampoule was placed in a two-zone furnace and the transport was carried out for 7 days at a source-zone temperature of 900°C and growth-zone temperature of 750°C. The resulting crystals were typically bulky with dimensions of about $10 \times 1.5 \times 0.1$ mm^3. They were transparent but slightly pink due to the Mn-induced absorption band[4] and exhibited p-type conductivity with resistivity of $2 \times 10^5\ \Omega$ cm. These as-grown crystals were used for the fabrication of the MSM diode.

*Present address: Mobara Works, Hitachi Ltd., Mobara, Chiba 297, Japan

2.2 *EL device fabrication*

2.2.1 *MSM diode*

The platelet-shaped crystal had well-developed {112} mirror-like surfaces with a thickness of 0.17 mm. The surface of the $CuAlS_2$:Mn single crystal was etched using HNO_3 solution. Circular Al disk films of 1 mm in diameter, as shown in Fig. 1, were deposited on both sides of the crystal as electrodes. The Au wires were connected to these by silver paste.

2.2.2 *PEL device*

The PEL device, shown schematically in Fig. 2, was prepared in the following manner. Shinetsu-Cyanoresin and propylene carbonate with a weight ratio of 1 : 3 were used as binder and solvent, respectively. The weight ratio of the phosphor and binder mixture was 6 : 1.

An indium-tin-oxide (ITO) was deposited by a DC sputtering method on a HOYA NA-40 glass substrate. The powder phosphor-binder mixture was spread on the surface of the ITO layer. The thickness of the EL phosphor-binder layer was 30–50 μm. The powder phosphor-binder mixture was then dried for 2 h at 72°C. Finally, the Al film was deposited on the phosphor-binder layer as a rear electrode.

2.3 *Measurements*

AC and DC voltages were applied between the electrodes of the MSM diode and the PEL device at room temperature. The position of the EL was observed by an optical stereo microscope. The *L–V* and the *L–I* characteristics were measured by an Advantest TQ-8210 photometer. The maximum luminance was measured by a Minolta ft-1-p luminance meter. The emitted light was dispersed by a Spex 1702 monochromator and detected by a Hamamatsu R928 photomultiplier. The EL-decay characteristics were measured with the help of a Tektoronix TDS 460 digital oscilloscope for averaging the photosignal.

3. Results

3.1 *EL characteristics of the MSM diode*

3.1.1 *Observation of the EL*

DC-EL was observed in the MSM diode using $CuAlS_2$:Mn. The DC-EL was more stable than the AC-EL.[5]

Observations using a stereo microscope revealed that the position in the cross-sectional plane, where the red EL occurred, was always on the positive electrode side on the surface of the crystal and moved to the opposite side when the polarity of the DC applied voltage was changed.

3.1.2 *EL spectrum*

The DC-EL spectrum of the MSM diode is shown in Fig. 3. The EL spectrum consists of a single broad band located in a pure red region. The peak wavelength is about 635 nm. The chromaticity diagram of the EL is shown in Fig. 4. The CIE color coordinates of the $CuAlS_2$:Mn EL device are X=0.66 and Y=0.34.

The DC-EL spectrum of the MSM diode had not changed from the photoluminescence (PL)[4] and the AC-EL[5] spectra observed previously in the single crystal. This suggests that the same luminescent center is involved in the DC-EL. In our previous studies, the PL band was assigned to the ligand-field transition from the lowest excited state ($^4T_1$) to the ground state ($^6A_1$) in the $3d^5$ manifold of the Mn^{2+} ion on the basis of photoluminescence excitation (PLE) studies.[4] The DC-EL is therefore also considered to be due to this d-d transition of the Mn^{2+} center.

3.1.3 *L–V, I–V and L–I characteristics*

Figure 5 illustrates the *L–V* and *I–V* curves of the MSM diode using $CuAlS_2$:Mn for a DC applied voltage. In this figure, the absolute scale of luminance is not given because the EL occurred behind the opaque electrode and was only observable in the peripheral region surrounding the circular

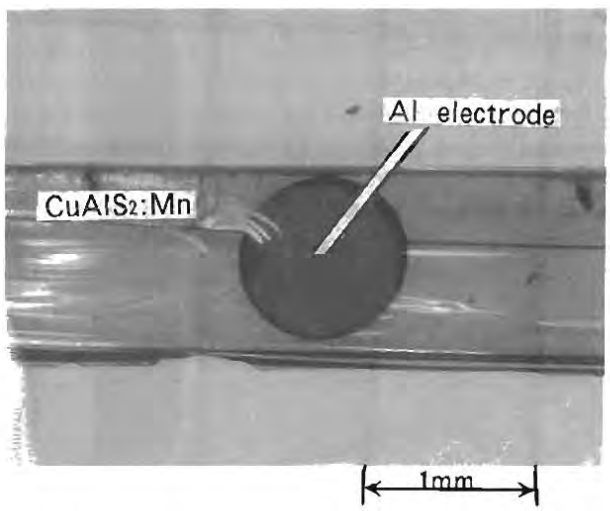

Fig. 1. Micrograph of Al–$CuAlS_2$:Mn–Al diode using a single crystal.

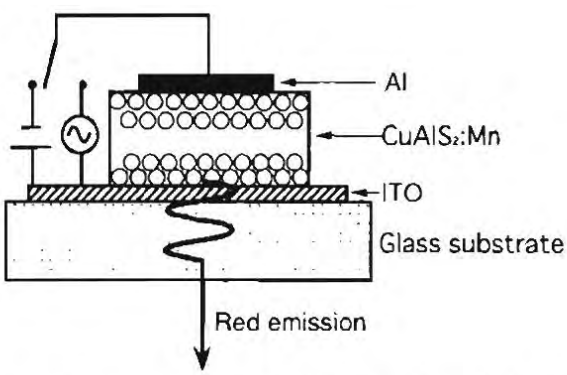

Fig. 2. Schematic illustration of powder EL device using $CuAlS_2$:Mn.

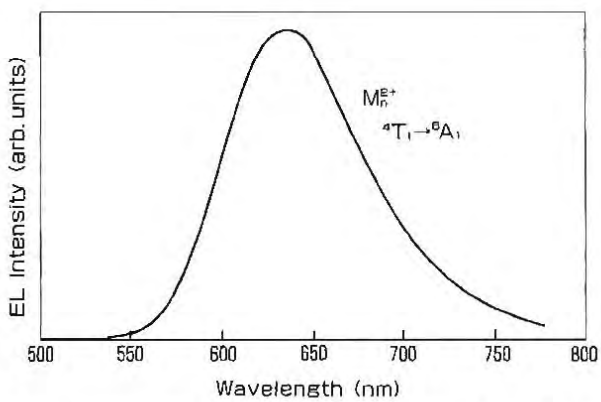

Fig. 3. DC-electroluminescence (EL) spectrum in Al–$CuAlS_2$:Mn–Al diode at room temperature.

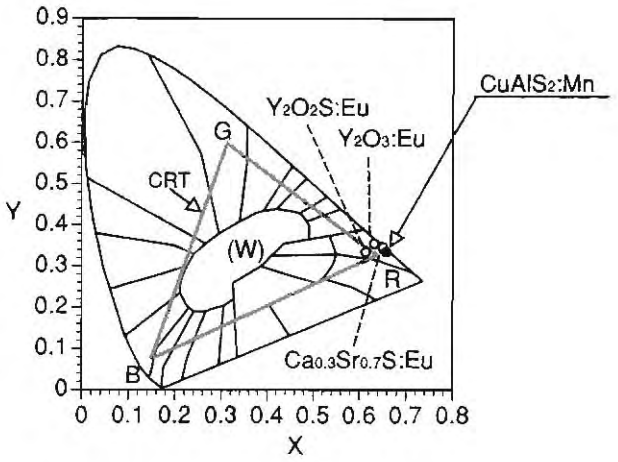

Fig. 4. CIE chromaticity diagram of powder EL devices ($CuAlS_2$:Mn, $Ca_{0.3}Sr_{0.7}S$:Eu) and CRT phosphors (Y_2O_2S:Eu, Y_2O_3:Eu).

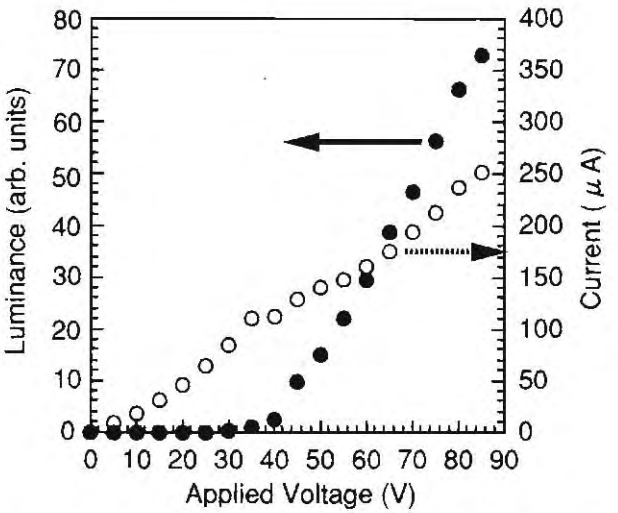

Fig. 5. Luminance–voltage (L–V) and current–voltage (I–V) characteristics of red DC-EL in an Al–$CuAlS_2$:Mn–Al diode at room temperature.

electrode. The luminance rapidly increases above the threshold voltage of 35 V. On the other hand, the current gradually increases with the applied voltage, and shows no threshold voltage. This I–V characteristic cannot be represented by a straight line due to the presence of some structures.

Figure 6 shows an L–I curve of the MSM diode. The luminance rapidly increases as current increases above the threshold current of 100 μA.

3.1.4 EL decay characteristics

Figure 7 shows oscilloscope trace of the applied pulse voltage, the EL intensity and the device current in the MSM diode. The red EL and the device current rise immediately after switching on the voltage, reaching saturation in a few μs. The emission and the current intensities remain constant during the period that the voltage is applied. Switching off the voltage causes only a relatively slow decrease of the EL in spite of the rapid decay of the device current.

Figure 8 shows the decay curve on the semilogarithmic scale of the EL in the MSM diode using a 1 wt% Mn-doped crystal. The decay time constant τ is determined to be 84.3 μs. Faster decay components with τ = 32.6 μs and 14.7 μs are also observed.

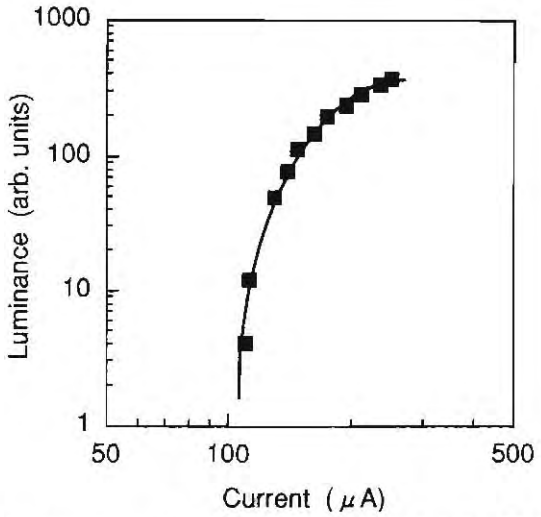

Fig. 6. Luminance–current (L–I) characteristics of red DC-EL in an Al $CuAlS_2$:Mn–Al diode at room temperature.

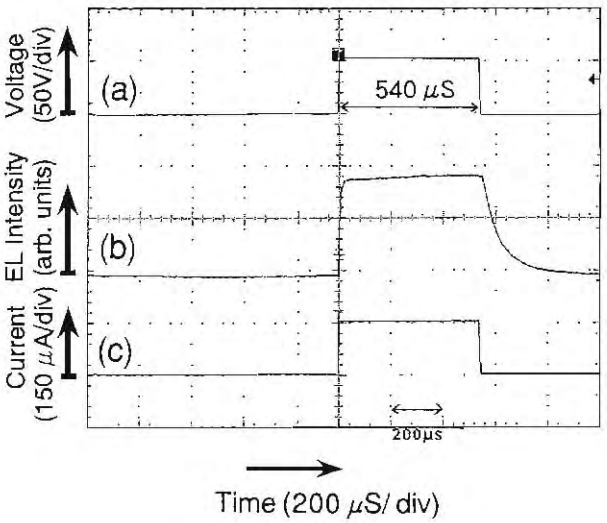

Fig. 7. Oscilloscope trace of the waveforms of red EL observed in an Al–$CuAlS_2$:Mn–Al diode. The horizontal time scale is 200 μs/div. (a) Applied pulse voltage. (b) Intensity of red EL. (c) Device current of the diode.

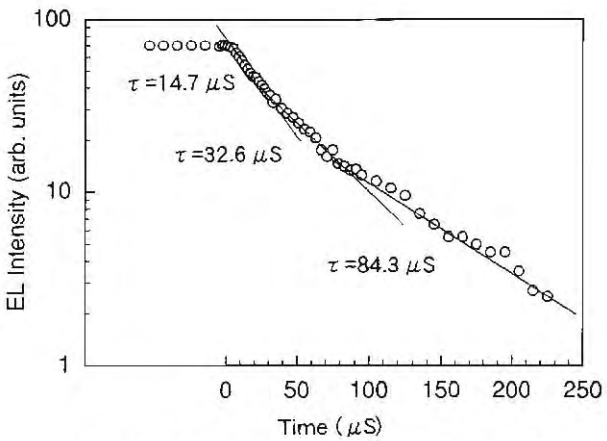

Fig. 8. A semilogarithmic plot of the decay curve of red EL in an Al–$CuAlS_2$:Mn–Al diode.

3.2 *Powder EL*

DC-EL of the PEL device using $CuAlS_2$:Mn was observed without the forming process necessary for conventional DC-powder EL devices.

Figure 9 illustrates the L–V curve of the red emission on the application of DC and AC voltages.

For an applied DC voltage, the EL luminance with *(1) the ITO positive and the Al negative* was about 10 times brighter than that with *(2) the ITO negative and the Al positive*. The maximum luminance for *(1)* was 0.2 cd/m^2.

For an applied AC voltage, when the voltage was over 80 V, the EL device became unstable and often suffered local breakdowns. The AC-EL luminance gradually became saturated on increasing the driving frequency to over 5 kHz.

The AC-EL was observed at the leading edge of the voltage, and the EL intensity did not change in the alternating voltage conditions between *(1) the ITO positive* and *(2) the ITO negative*.

Comparing the DC-EL and the AC-EL for the same value of applied voltage, the DC-EL was about 10 times as bright as the AC-EL.

4. Discussion

4.1 *MSM diode*

4.1.1 *EL excitation mechanism*

In general, two types of excitation mechanisms for the excitation of DC-EL using luminescent centers are proposed, namely the light-emitting diode (LED) and high-field EL modes. The LED mode is always observed in the DC-diode, utilizing emissions from luminescent centers excited through energy transfer by the recombination of injected minority carriers.[6,7] On the other hand, the high-field EL mode, which is often observed in DC and AC thin film EL devices, utilizes emissions from luminescent centers excited by hot majority carriers.[8,9] In this section, it is considered whether the DC-EL of $CuAlS_2$:Mn is in the LED or high-field EL mode.

As shown in Fig. 5, the field strength of the emission threshold is as high as 2.0×10^5 V/m, as estimated from the threshold voltage and the crystal thickness assuming uniform field distribution. The emission is observed on the surface of the crystal, where a relatively high field is supposed to be concentrated. The field is expected to be several orders of magnitude larger than 2.0×10^5 V/m and the EL to be related to hot carrier excitation.

In the usual DC-MSM diode using ZnS host crystals, it is experientially well known that the luminance L is given by the following equation:[8,10]

$$L = L_0 \times \exp(-B/\sqrt{V}) \tag{1}$$

where L_0 and B are constants, and V is the applied voltage.

In Fig. 10, the luminance values obtained experimentally are plotted as squares against the inverse square root of the applied voltage on a semilogarithmic scale. It is found that the experimental data fits eq. (1), indicated by the straight line in the figure. This result suggests that the EL is caused by a similar excitation mechanism as that in ZnS host crystals, which is categorized as high-field EL.

Figure 6 shows the L–I curve of the MSM diode. In usual LED type EL, when a voltage of 1–3 V is applied, a linear relationship holds in the log-log plot between luminance and current, and no threshold behavior is observed.[6] In our MSM diode, the L–I curve has a threshold current of 100 μA and eventually L becomes saturated with the increase in current. We conclude from these L–I characteristics that the emission is caused by hot carrier excitation.

Thus, both the L–V and the L–I curves lead us to the conclusion that the Mn^{2+} ions are not excited by the recombination of injected minority carriers but by high-field accelerated hot carriers. We propose the energy band model shown in Fig. 11, by considering the I–V characteristics observed in the single crystal.

A current density originating from carriers which emit through a triangular barrier formed by a high electric field of over 10^8 V/m generally obeys the Fowler-Nordheim (FN) form, in which current density J is expressed as[11]

$$J \approx E^2 \cdot \exp[-8\pi\sqrt{2\pi}(e\phi)^{3/2}/3ehE]$$
$$\approx V^2 \cdot \exp(-A \cdot \phi^{3/2} d/V) \tag{2}$$

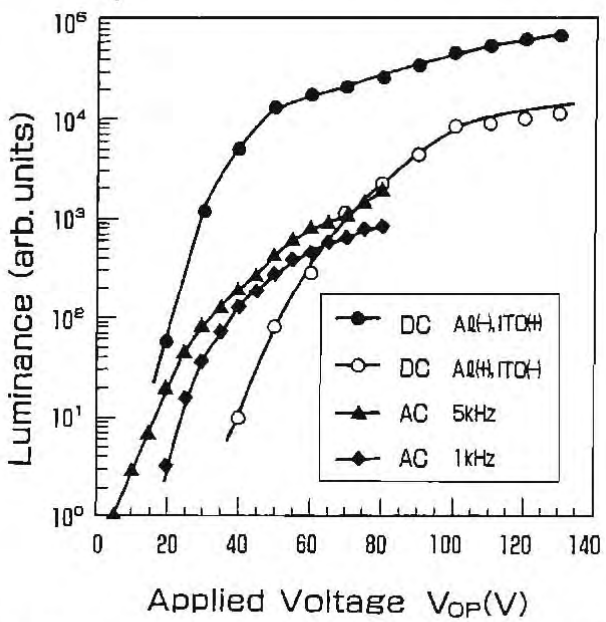

Fig. 9. Luminance–voltage (L–V) characteristics of red AC- and DC-EL in powder EL device using $CuAlS_2$:Mn at room temperature.

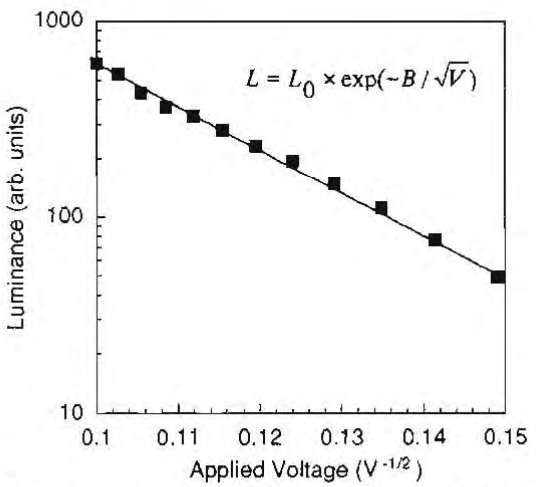

Fig. 10. Semilogarithmic plot of relationship between red EL luminance and inverse of square root applied voltage. The black squares are experimental points and the solid line the best fit to eq. (1).

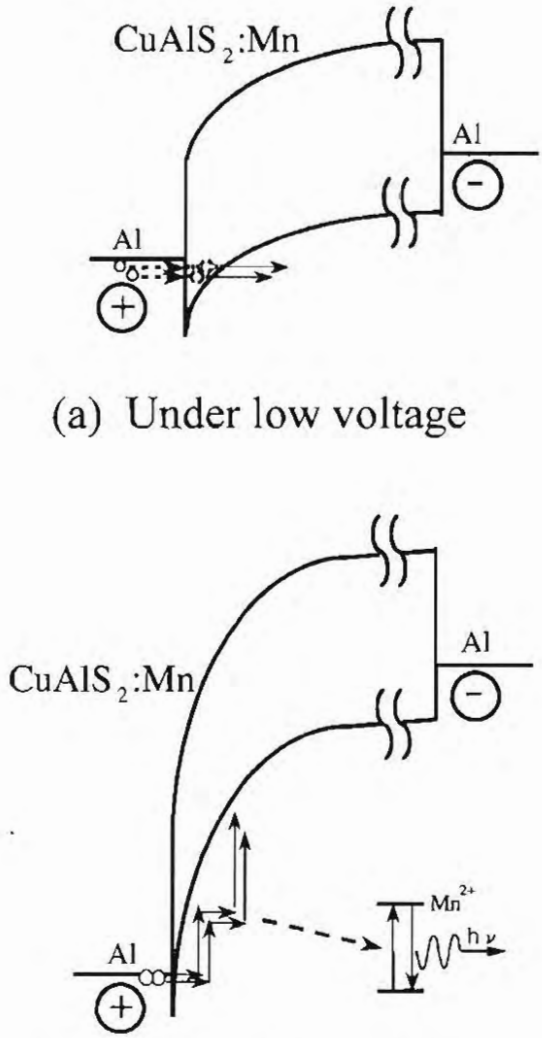

Fig. 11. Tentative energy band diagram for DC voltage applied to an Al–$CuAlS_2$:Mn–Al diode and the EL excitation mechanism. (a) Under low voltage ($V < 35$ V). (b) Under high voltage ($V > 35$ V).

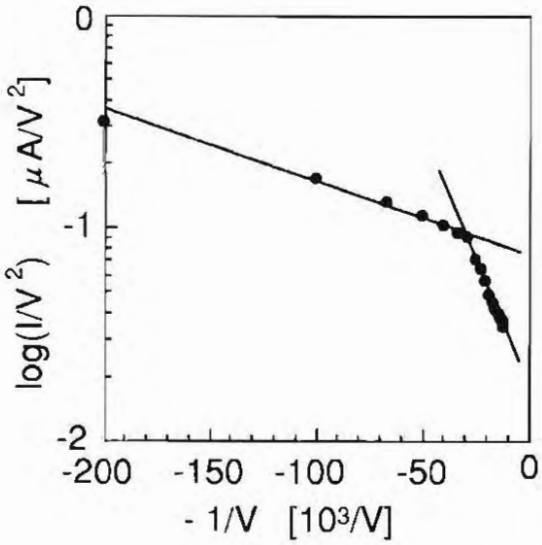

Fig. 12. Fowler-Nordheim (FN) plot of I–V characteristics for DC voltage applied to an Al–$CuAlS_2$:Mn–Al diode.

where e is the unit of electronic charge, h is Planck's constant, ϕ the barrier height, m the carrier effective mass, E the electric field, V the applied voltage, d the barrier width, and A is a constant. This current mode is theoretically expected to be characterized by the FN plot, which implies that a plot of $\log(I/V^2)$ against $-1/V$ follows a straight line. It follows from eq. (2) that the slope of the straight line is approximately linear with $\phi^{3/2} \cdot d$.

Figure 12 shows the actual FN plot of $CuAlS_2$:Mn derived from the I–V characteristics shown in Fig. 5. This FN plot clearly consists of two linear sections which obey the FN form. The $-1/V$ value at the intersection of the two straight lines is -0.0286 (1/V), and this value is equivalent to an applied voltage of $V = 35$ V which itself clearly corresponds to the threshold voltage of the EL.

From Fig. 12, for low applied voltages [$-1/V < -0.0286$ (1/V), namely $V < 35$ V] where the EL is not observed, the small value of the slope suggests that the device current is mainly due to field emission from the trap level where carriers tunnel through a potential barrier. For the origin of the tunnel current, the hole emission from an acceptor level is regarded as the most promising mechanism for the following reasons.

(1) $CuAlS_2$:Mn has an acceptor level due to p-type conductivity. The activation energy of the acceptor level is constant during the change of the applied voltage V in the range of 0–35 V, which satisfies eq. (2).
(2) The majority carriers of $CuAlS_2$:Mn are holes due to p-type conductivity.
(3) In $CuAlS_2$:Mn, the EL always occurs on the positive electrode side. On the other hand, in the ZnS:Cu crystal exhibiting the n-type with electron conduction, EL occurs on the negative electrode side.[10]
(4) Taking account of the fact that the EL is always observed on the positive electrode side, the electric field should be enlarged near the positive electrode even for low applied voltages ($V < 35$ V), as shown in Fig. 11(a). The main carriers for the emission current should therefore be holes emitted from the acceptor level where holes are injected from the positive electrode by the concentrated electric field, and not electrons injected from the negative electrode due to the lower electric field on the negative electrode side and due to the very long drift distance (~0.17 mm) equivalent to the crystal's thickness.

At a higher applied voltage [$-1/V > -0.0286$ (1/V), namely $V > 35$ V], where the EL is observed, the slope of the FN plot is about 8 times steeper, as shown in Fig. 12. Another type of field emission therefore occurs at higher applied voltages ($V > 35$ V) where the accelerated carriers tunnel directly through the higher barrier ϕ_{EL}. It is thought that band bending in the $CuAlS_2$:Mn crystal exceeds the transparency of the triangular barrier at the boundary of the $CuAlS_2$:Mn–Al interface, as shown in Fig. 11(b). As $CuAlS_2$:Mn shows p-type conductivity, directly injected holes from the positive electrode are sufficiently accelerated by the high electric field and become hot holes which enables EL excitation.

The barrier height for the EL is estimated to be $\phi_{EL} = 0.78$ eV, using eq. (2) with the parameters that the slope of the FN plot for the higher applied voltage ($V > 35$ V) is about 8 times steeper than that for the lower applied volt-

ages ($V < 35$ V) as shown in Fig. 12, the barrier width d is always constant, and the activation energy for the acceptor level is $E_A = 0.19$ eV[12] which is the value obtained from the undoped $CuAlS_2$ and is tentatively used for the Mn-doped sample.

4.1.2 EL chromaticity

Figure 4 shows the color coordinates of representative red phosphors, i.e. Y_2O_2S:Eu (X=0.61 and Y=0.34)[13] and Y_2O_3:Eu (X=0.63 and Y=0.36)[13] for CRT, and $Ca_{0.3}Sr_{0.7}S$:Eu (X=0.65 and Y=0.35)[2] for the newly reported PEL device. The EL of $CuAlS_2$:Mn also has pure red color coordinates similar to those of CRT. The CIE color coordinates (X=0.66 and Y=0.34) of $CuAlS_2$:Mn EL are sufficient for use as the red-PEL phosphor of a full-color device.

4.1.3 EL decay characteristics

The slow decay times observed in the decay curve of the EL shown in Fig. 8 seem to reflect the forbidden nature of d-d transition in the Mn^{2+} ion. The observed decay times ($\tau = 84.3\,\mu$s, 32.6 μs and 14.7 μs) show relatively good correspondence to the previously reported PL decay times ($\tau = 133\,\mu$s, 53 μs and 22 μs) in $CuAlS_2$:Mn with the same Mn concentration.[14] In the PL experiments, it was found that the maximum decay time was about 1.3–1.4 ms in 0.01 wt% Mn-doped samples, while it decreases to 133 μs in the 1 wt% Mn-doped sample. For faster decay, the shortening of decay times was attributed to the formation of Mn–Mn pairs. We conclude that the EL decay time $\tau = 84.3\,\mu$s corresponds to Mn–Mn pairs, while the other two shorter decay times involve the coupling of Mn–Mn pairs with other impurity/defect centers.

4.2 Powder EL

In the DC-EL of the PEL phosphor using ZnS as the host material, a forming process is generally necessary to obtain the EL, and this process becomes troublesome for the fabrication of practical EL devices.[15] On the other hand, PEL device using $CuAlS_2$:Mn emits even in the absence of the forming process. This indicates that with $CuAlS_2$:Mn it is relatively easy to form a high electric field on the surface of the crystal itself.

Under DC voltage, the luminance in the applied voltage condition of *(1) ITO positive and Al negative* is brighter than that of *(2) ITO negative and Al positive*. This can be explained by the fact that the emitting position of the EL phosphor always occurs on the positive electrode side, which has been confirmed by the observation of the emitting position in the single crystal as described in §3.1.1. For *(1) ITO positive*, the EL occurs on the ITO side of the powder phosphor, and for *(2) ITO negative*, the EL occurs on the Al side of the powder phosphor. The luminance in *(1)* is therefore brighter than that in *(2)*.

In addition, the different barrier heights between the ITO–$CuAlS_2$:Mn and Al–$CuAlS_2$:Mn interfaces affect carrier acceleration, which may lead to asymmetric EL intensities depending upon the polarity of the applied voltages.

From the L–V characteristics shown in Fig. 9, the luminance of the DC-EL is brighter than that of the AC-EL. The reason for this is as follows.

It is obvious that the DC-EL continues during the application of DC voltage. On the other hand, the AC-EL occurs only when the polarity of the AC voltage waveform is reversed. Essentially, the luminance of AC-EL usually increases in proportion to the driving frequency.

As described in §3.2, however, the luminance of the PEL device using $CuAlS_2$:Mn gradually becomes saturated above a driving frequency of around 5 kHz. It is supposed that this luminance saturation is due to the slow decay of Mn^{2+} ions. The driving frequency f_{LS} at which the luminance saturation begins can be estimated using the decay time τ of Mn^{2+} ions. Since the number of the emitting times per one driving cycle is twice that on the positive and negative sides of the applied voltage waveforms, f_{LS} is given by:

$$f_{LS} \approx 1/(\tau \times 2). \tag{3}$$

Thus, f_{LS} is estimated to be 5.9 kHz, using eq. (3) with $\tau = 84.3\,\mu$s. As the driving frequency increases from around 5 kHz, the Mn^{2+} ion emissions pile up, and the luminance gradually saturates.

In this saturated AC-EL operation, the AC voltage alternates between *(1) ITO positive and (2) ITO negative*. As described in §3.2, the AC-EL intensity does not change in these alternating voltage conditions. This indicates that the AC-EL does not occur at the ITO–$CuAlS_2$:Mn or Al–$CuAlS_2$:Mn interfaces but in the widely dispersed $CuAlS_2$:Mn powder in the phosphor-binder layer. The emitting position of $CuAlS_2$:Mn powder is therefore mainly distant from the ITO electrode, and the EL intensity is weak.

On the other hand, the DC-EL always occurs at the ITO-$CuAlS_2$:Mn interface under the condition of *(1) ITO positive*, so that brighter emission on the ITO side is continuously maintained. The brighter DC-EL performance is therefore explained by the emitting position in the phosphor-binder layer.

5. Conclusions

EL of the Mn-doped $CuAlS_2$ single crystal has been carefully investigated. It is concluded from the L–V, I–V and L–I curves that the EL is excited by hot holes. The EL of $CuAlS_2$:Mn has pure red color coordinates similar to those of CRT. The EL shows a slow decay with a time constant $\tau = 84.3\,\mu$s. Taking account of the high Mn concentration (1 wt%), the slow decay times are attributed to the Mn–Mn pairs.

A PEL device using $CuAlS_2$:Mn has been fabricated for the first time. Under DC applied voltage, the PEL device began to emit in the absence of the forming process which is necessary for the conventional powder EL device. The luminance of the DC-EL was brighter than that of the AC-EL. This higher luminance is explained by the emitting position in the phosphor-binder layer.

Acknowledgments

The authors express their sincere gratitude to Professor N. Koshida for helpful suggestions.

1) Y. A. Ono: *Electroluminescent Displays* (World Scientific, Singapore, 1995) p. 7.
2) A. Uemura, H. Kobayashi, M. Kimura and H. Ohnishi: Dig. Int. Conf. IDW96, (International Display Workshops), Kobe, 1996. p. 89.
3) S. Shirakata, I. Aksenov, K. Sato and S. Isomura: Jpn. J. Appl. Phys. 31 (1992) L1071.
4) K. Sato, S. Okamoto, M. Morita, A. Morita, T Kambara and H. Takenoshita: Prog. Cryst. Growth & Char. 10 (1984) 311.
5) K. Sato, K. Ishii, K. Tanaka, S. Matsuda and S. Mizukawa: *Electrolumi-*

nescence, eds. S. Shionoya and H. Kobayashi (Springer, Berlin, 1989) p. 390.
6) J. I. Pankove: *Electroluminescence* (Springer, New York, 1977) p. 166.
7) G. M. Ford and B. W. Wessels: Appl. Phys. Lett. **68** (1996) 19.
8) J. I. Pankove: *Electroluminescence* (Springer, New York, 1977) p. 159.
9) T. Mishima, W. Quan-kun and K. Takahashi: J. Appl. Phys. **52** (1981) 5797.
10) A. Vecht and N. J. Werring: J. Phys. D **3** (1970) 105.
11) *Handbook of Phosphor*, eds. S. Shionoya (Ohmsha, Tokyo, 1987) p. 87 [in Japanese].
12) I. Aksenov, N. Nishikawa and K. Sato: J. Appl. Phys. **74** (1993) 3811.
13) *Handbook of Phosphor*, eds. S. Shionoya (Ohmsha, Tokyo, 1987) p. 279 [in Japanese].
14) K. Sato, K. Ishii, K. Watanabe and K. Ohe: Jpn. J. Appl. Phys. **30** (1991) 307.
15) Y. A. Ono: *Electroluminescent Displays* (World Scientific, Singapore, 1995) p. 12.